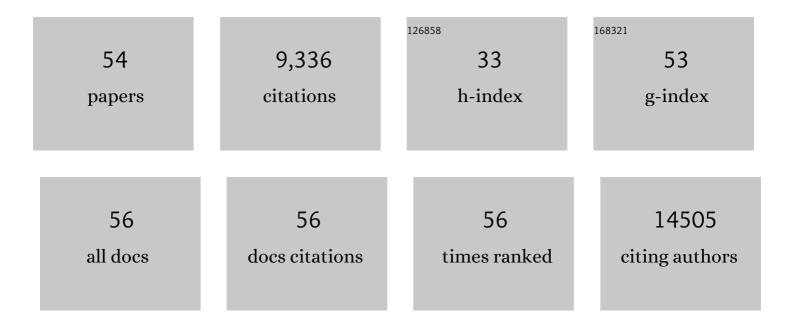
Jiangtian Li

List of Publications by Year in descending order

Source: https://exaly.com/author-pdf/4601260/publications.pdf Version: 2024-02-01



#	Article	lF	CITATIONS
1	Nanostructured carbon–metal oxide composite electrodes for supercapacitors: a review. Nanoscale, 2013, 5, 72-88.	2.8	1,853
2	Photocatalytic Activity Enhanced by Plasmonic Resonant Energy Transfer from Metal to Semiconductor. Journal of the American Chemical Society, 2012, 134, 15033-15041.	6.6	1,052
3	Semiconductor-based photocatalysts and photoelectrochemical cells for solar fuel generation: a review. Catalysis Science and Technology, 2015, 5, 1360-1384.	2.1	824
4	Solar Hydrogen Generation by Nanoscale <i>p–n</i> Junction of <i>p</i> -type Molybdenum Disulfide/ <i>n</i> -type Nitrogen-Doped Reduced Graphene Oxide. Journal of the American Chemical Society, 2013, 135, 10286-10289.	6.6	599
5	Plasmon-induced resonance energy transfer for solar energy conversion. Nature Photonics, 2015, 9, 601-607.	15.6	587
6	Solar Hydrogen Generation by a CdS-Au-TiO ₂ Sandwich Nanorod Array Enhanced with Au Nanoparticle as Electron Relay and Plasmonic Photosensitizer. Journal of the American Chemical Society, 2014, 136, 8438-8449.	6.6	533
7	Ag@Cu ₂ O Core-Shell Nanoparticles as Visible-Light Plasmonic Photocatalysts. ACS Catalysis, 2013, 3, 47-51.	5.5	471
8	Plasmon-induced photonic and energy-transfer enhancement of solar water splitting by a hematite nanorod array. Nature Communications, 2013, 4, 2651.	5.8	427
9	Single-crystalline Ni(OH)2 and NiO nanoplatelet arrays as supercapacitor electrodes. Nanoscale, 2011, 3, 5103.	2.8	287
10	Water-Soluble Superparamagnetic Magnetite Nanoparticles with Biocompatible Coating for Enhanced Magnetic Resonance Imaging. ACS Nano, 2011, 5, 6315-6324.	7.3	250
11	Photocatalytic Water Oxidation by Hematite/Reduced Graphene Oxide Composites. ACS Catalysis, 2013, 3, 746-751.	5.5	226
12	Controlling Plasmon-Induced Resonance Energy Transfer and Hot Electron Injection Processes in Metal@TiO ₂ Core–Shell Nanoparticles. Journal of Physical Chemistry C, 2015, 119, 16239-16244.	1.5	219
13	Boosted Oxygen Evolution Reactivity by Igniting Double Exchange Interaction in Spinel Oxides. Journal of the American Chemical Society, 2020, 142, 50-54.	6.6	199
14	Photoelectrochemical performance enhanced by a nickel oxide–hematite p–n junction photoanode. Chemical Communications, 2012, 48, 8213.	2.2	196
15	Template-Free Preparation of Mesoporous Fe ₂ O ₃ and Its Application as Absorbents. Journal of Physical Chemistry C, 2008, 112, 13378-13382.	1.5	140
16	Enhancement of Solar Hydrogen Generation by Synergistic Interaction of La ₂ Ti ₂ O ₇ Photocatalyst with Plasmonic Gold Nanoparticles and Reduced Graphene Oxide Nanosheets. ACS Catalysis, 2015, 5, 1949-1955.	5.5	122
17	Oxygen Evolution Reaction in Energy Conversion and Storage: Design Strategies Under and Beyond the Energy Scaling Relationship. Nano-Micro Letters, 2022, 14, 112.	14.4	104
18	Microsomal Glutathione Transferase 1 Protects Against Toxicity Induced by Silica Nanoparticles but Not by Zinc Oxide Nanoparticles. ACS Nano, 2012, 6, 1925-1938.	7.3	100

Jiangtian Li

#	Article	IF	CITATIONS
19	Enhanced photoelectrochemical activity of an excitonic staircase in CdS@TiO2 and CdS@anatase@rutile TiO2 heterostructures. Journal of Materials Chemistry, 2012, 22, 20472.	6.7	87
20	Photocatalytic generation of hydrogen with visible-light nitrogen-doped lanthanum titanium oxides. Catalysis Today, 2013, 199, 48-52.	2.2	85
21	A facile route to synthesize magnetic particles within hollow mesoporous spheres and their performance as separable Hg2+ adsorbents. Journal of Materials Chemistry, 2008, 18, 2733.	6.7	74
22	Photoelectrochemical overall water splitting with textured CuBi ₂ O ₄ as a photocathode. Chemical Communications, 2018, 54, 3331-3334.	2.2	72
23	SnO2@CdS nanowire-quantum dots heterostructures: tailoring optical properties of SnO2 for enhanced photodetection and photocatalysis. Nanoscale, 2013, 5, 3022.	2.8	69
24	Differential Mouse Pulmonary Dose and Time Course Responses to Titanium Dioxide Nanospheres and Nanobelts. Toxicological Sciences, 2013, 131, 179-193.	1.4	64
25	Ru@RuO ₂ Coreâ€5hell Nanorods: A Highly Active and Stable Bifunctional Catalyst for Oxygen Evolution and Hydrogen Evolution Reactions. Energy and Environmental Materials, 2019, 2, 201-208.	7.3	64
26	Preparation and visible-light photocatalytic activity of In2S3/TiO2 composite. Materials Chemistry and Physics, 2010, 122, 183-187.	2.0	62
27	Study of the inorganic substitution in a functionalized UiO-66 metal–organic framework. Physical Chemistry Chemical Physics, 2016, 18, 12748-12754.	1.3	61
28	Functionalization of a Metal-Organic Framework Semiconductor for Tuned Band Structure and Catalytic Activity. Journal of the Electrochemical Society, 2019, 166, H3029-H3034.	1.3	44
29	Distorted Inverse Spinel Nickel Cobaltite Grown on a MoS ₂ Plate for Significantly Improved Water Splitting Activity. Chemistry of Materials, 2019, 31, 7590-7600.	3.2	42
30	Electron transport properties of an ethanol-soluble AlQ3-based coordination polymer and its applications in OLED devices. Journal of Materials Chemistry, 2009, 19, 4551.	6.7	39
31	A one-pot method to grow pyrochlore H4Nb2O7-octahedron-based photocatalyst. Journal of Materials Chemistry, 2010, 20, 1942.	6.7	38
32	Linear and nonlinear optical properties of covalently bound C.I. Disperse Red 1 chromophore/silica hybrid film. Dyes and Pigments, 2008, 78, 219-224.	2.0	35
33	Air-processed depleted bulk heterojunction solar cells based on PbS/CdS core–shell quantum dots and TiO2 nanorod arrays. Solar Energy Materials and Solar Cells, 2014, 124, 67-74.	3.0	35
34	Preparation and DSC application of the size-tuned ZnO nanoarrays. Journal of Alloys and Compounds, 2010, 489, 694-699.	2.8	26
35	Distinguishing surface effects of gold nanoparticles from plasmonic effect on photoelectrochemical water splitting by hematite. Journal of Materials Research, 2016, 31, 1608-1615.	1.2	25
36	Multimetallic FeCoNiO _{<i>x</i>} Nanoparticles Covered with Nitrogen-Doped Graphene Layers as Trifunctional Catalysts for Hydrogen Evolution and Oxygen Reduction and Evolution. ACS Applied Nano Materials, 2020, 3, 7119-7129.	2.4	24

Jiangtian Li

#	Article	IF	CITATIONS
37	Donor–π–acceptor structure between Ag nanoparticles and azobenzenechromophore and its enhanced third-order optical non-linearity. Dalton Transactions, 2009, , 823-831.	1.6	23
38	A soluble coordination polymer and its sol–gel-derived amorphous films: synthesis and third-order nonlinear optical properties. Journal of Materials Chemistry, 2008, 18, 3688.	6.7	19
39	An easy co-casting method to synthesize mesostructured carbon composites with high magnetic separability and acid resistance. New Journal of Chemistry, 2009, 33, 1926.	1.4	18
40	Earth-Abundant Fe and Ni Dually Doped Co ₂ P for Superior Oxygen Evolution Reactivity and as a Bifunctional Electrocatalyst toward Renewable Energy-Powered Overall Alkaline Water Splitting. ACS Applied Energy Materials, 2021, 4, 9969-9981.	2.5	18
41	Room-temperature ferromagnetism in Ti1â^'V O2 nanocrystals synthesized from an organic-free and water-soluble precursor. Journal of Alloys and Compounds, 2010, 499, 160-165.	2.8	16
42	Understanding charge transfer dynamics in QDs-TiO2 nanorod array photoanodes for solar fuel generation. Applied Surface Science, 2018, 429, 48-54.	3.1	16
43	Energy band engineering of metal oxide for enhanced visible light absorption. , 2018, , 49-78.		16
44	Preparation and third-order optical nonlinearity of gold nanoparticles incorporated mesoporous TiO_2 thin films. Journal of the Optical Society of America B: Optical Physics, 2009, 26, 107.	0.9	14
45	Stepwise in situ synthesis and characterization of metallophthalocyanines@mesoporous matrix SBA-15 composites. Physical Chemistry Chemical Physics, 2010, 12, 5109.	1.3	9
46	Thermodynamics of the oxygen evolution electrocatalysis in a functionalized UiOâ€66 metalâ€organic frameworks. International Journal of Quantum Chemistry, 2016, 116, 1153-1159.	1.0	9
47	Seamless separation of OH _{ad} and H _{ad} on a Ni–O catalyst toward exceptional alkaline hydrogen evolution. Journal of Materials Chemistry A, 2022, 10, 1278-1283.	5.2	9
48	A two-step surface modification approach for Au and CdS NPs loaded mesoporous thin films and the greatly enhanced optical nonlinearity. Dalton Transactions, 2010, 39, 3233.	1.6	7
49	Azo Chromophore Monomerically Bonded Mesostructured Silica Films with Large Third-Order Nonlinearity but Negligible Nonlinear Absorption. Journal of Physical Chemistry C, 2008, 112, 13754-13762.	1.5	6
50	A pre-modification-direct synthesis route for the covalent incorporation and monomeric dispersion of hydrophobic organic chromophores in mesoporous silica films. Microporous and Mesoporous Materials, 2008, 111, 150-156.	2.2	3
51	Diazobenzene chromophore-doped silica films with large two-photon absorption cross-section. Dyes and Pigments, 2009, 82, 204-208.	2.0	3
52	Carbon nanostructures formed on mesoporous silica by catalytic chemical vapor deposition of ethene. Journal of Materials Research, 2008, 23, 435-443.	1.2	2
53	Above and below band edge light recovery with plasmonics. Proceedings of SPIE, 2015, , .	0.8	2
54	Dual Roles of MoO3 Thin Film in Improving the Performance of Copper Bismuth Oxide Photocathode for Solar Water Splitting. Journal of Electrochemical Energy Conversion and Storage, 2020, 17, .	1.1	0